Fire behaviour of limestone masonry during and after fire

Pierre Pimienta, Armita Obaie, Elodie Donval, Toan Duc, Albert Noumowe, Javad Eslami, Dashnor Hoxha

FIRE BEHAVIOUR OF LIMESTONE MASONRY DURING AND AFTER FIRE


Pierre Pimienta a,*


Armita Obaie b


Elodie Donval c


Duc Toan Pham d


Albert Noumowe e


Javad Eslami f


Dashnor Hoxha g

ABSTRACT

The work presented in this paper is part of a larger French project, POSTFIRE, developed following the Notre-Dame Cathedral fire. Six fire resistance tests were performed on 3 m x 3 m x 20 cm thick masonry walls. The tests were performed on 3 stones: Saint Leu (soft stone), Tervoux (firm stone) and Massangis (hard stone). The nature and compressive strength of the mortars were adapted to each stone. The walls were exposed to the standard 834-1 temperature curve for two hours followed by a 24-hour cooling phase. For each stone, one wall was tested without mechanical loading and one with mechanical loading. The applied mechanical loads during the fire test correspond to 50% of the allowable loads calculated according to Eurocode 6. The tests were very extensively instrumented: thermocouples, displacement sensors, digital image correlation, thermal camera and endoscopes. The recordings were made during the heating and cooling phase. At the end of the cooling phase, the walls were loaded again until failure to determine their residual wall bearing capacity. The walls were stored for at least 2 weeks for further observations. The results of the test campaign on the 6 walls made with the 3 stones will be presented.

Keywords: Masonry; Limestone; Fire resistance; Cooling phase; Residual bearing capacity.

[a,*] CSTB (pierre.pimienta@cstb.fr), Corresponding author.
[b] L2MGC CY Cergy-Paris Université, Université d'Orléans, CSTB (armita.obaei@cyu.fr).
[c] CSTB (elodie.donval@cstb.fr).
[d] CSTB (ductoaan.pham@cstb.fr).
[e] L2MGC CY Cergy-Paris (albert.noumowe@cyu.fr).
[f] L2MGC CY Cergy-Paris (javad.eslami@cyu.fr).
[g] Université d'Orléans (dashnor.hoxha@univ-orleans.fr).

1. INTRODUCTION

Masonry construction has been used for centuries due to its durability and resistance to the elements. However, when exposed to fire, masonry structures can experience significant damage. The recent, devastating fire of Notre Dame de Paris has enlightened once more the vulnerability of historic architectural heritage and the general concern for the residual stability of the monument. As a fact, many ancient buildings and monuments have withstood violent fires during their history; structural masonry often survives fires. This can be explained by the generally high thickness of these structures and the tendency of the stones to show lower temperature degradation compared to other building materials. On the other hand, the residual structural capacity of masonry walls, pillars, columns and vaults is difficult to quantify [1]. Generally, only destructive tests (DT) can provide quantitative assessment of mechanical properties; but the need for heritage preservation generally forces post-fire surveyors to rely mainly upon non-destructive tests (NDT) [2]. On the other hand, even performance-based codes for the fire resistance assessment of masonry structures – like Eurocode [3] and the USA code NFPA 914 [4]– do not contain specific strength calculation methods for post-fire situation.

In the field of civil engineering, the high temperature behaviour of stones is much less known and investigated than that of steel or concrete. At high temperatures, microscopic physical and chemical transforms trigger macroscopic changes in the physical, thermal and mechanical properties of masonry units and mortars [5]. In carbonate rocks, e.g. limestone, decarbonisation is the cause for material contraction beyond 800°C, while the formation of Portlandite brings on a volume increase during the cooling phases [6] [7]. Damage increase can show up even days after the fire event [8],[9], having major consequences on the safety of buildings after fire.
Additionally, the composite nature of masonry brings on the problem of interface cohesion deterioration, which is a crucial parameter especially in the shear response [10]. Among the exposure characteristics, the maximum temperature is the most relevant parameter for the property decay [11]. As well, the cooling regime can also be crucial [12]. Finally, high heating rates (which are typical of real fires) can also be linked to damage increase and, depending on the stone nature, spalling [13].
Despite the importance of understanding how masonry behaves in fire situations and after the fire, the available research on these topics is limited and the very heterogeneous results claim for increasing scientific contributions. However, we can mention the work carried out at the CSTB (Centre Scientifique et Technique du Bâtiment) over the last few years, including the performance of fire resistance tests on masonry walls [14][15]. The tests were performed on Saint-Vaast limestone which is very close to the soft stone Saint Leu studied in the present paper. This work is currently being continued and includes detailed work on the modelling of the failure behavior under fire.

In this context, the French POSTFIRE project – *Safety and Preservation of cultural heritage stone masonry buildings after fire events* – aims at understanding and examine the multi-scale mechanical behaviour of traditional stonework, during the fire and, with a particular focus, after the fire. This project includes the carrying out of a fire resistance test campaign on the 6 walls in CSTB. This work also completes the ongoing research on Saint Vaast stones [14][15] which focuses mainly on the masonry behavior under fire and little on the behavior after cooling. The tests were very extensively instrumented: thermocouples, displacement sensors, digital image correlation, thermal camera and endoscopes. This paper presents the program, equipment, test procedures and the main tests results and analysis.

2. EXPERIMENTAL PROGRAM

In order to investigate the behavior of Limestone in fire situations, six masonry wall tests were conducted (Table 1). Tests were carried out on 3 m x 3 m x 20 cm thick masonry walls and performed on 3 three types of limestone from the French Rocamat company: Saint Leu (soft stone), Tervoux (firm stone) and Massangis (hard stone). Mean values of the stones compressive strengths achieved by testing 10 cubic 10 cm-side samples according to NF EN 772-1 are given in the table.

Table 1: Experimental program

Wall	Stone	Stone compressive strength (MPa)	Mortar	Mortar compressive strength (MPa)	Curing time (months)	Applied compressive load on the walls
LEU NL	Saint-Leu	7.3 ± 1	350 kg NHL2	Hor. : 0.67 Vert. : 0.65	4	Lightly loaded – 14 tonnes (0.23 MPa)
LEU L	Saint-Leu				4	Loaded – 36.3 tonnes (0.61 MPa)
TER NL	Tervoux	37.3 ± 1	250 kg NHL3.5 + 100 kg cement	Hor. : 1.5 Vert.: 1.75	2	Lightly Loaded– 30 tonnes (0.5 MPa)
TER L	Tervoux				2	Loaded – 141 tonnes (2.35 MPa)
MAS NL	Massangis	102.4 ± 6	200 kg NHL3.5 + 150 kg cement	6.7	3	Lightly Loaded – 26 tonnes (0.43 MPa)
MAS L	Massangis				3	Loaded – 375 tonnes (6.25 MPa)

The nature and compressive strength of the mortars were adapted to each stone. In order to reproduce site practices, the fluidity of the mortars, and therefore their water content, was adapted for the filling of horizontal and vertical joints. The water content of the mortars for vertical joints was higher (Table 1). Then, Saint-Leu stone was bonded with mortar made of sand and natural hydraulic lime NHL 2 with a compressive strength of 0.65 – 0.67 MPa. Mortars used for Tervoux and Massangis stones were made of sand, cement, and natural hydraulic lime NHL 3.5. Their compressive strengths was respectively 1.5 – 1.75 MPa and 6.7 MPa. The curing time was adapted to the strength kinetics of the mortars. A longer curing time (4 months) was applied for the Saint-Leu limestone walls bonded with the mortar made with natural hydraulic lime NHL 2.
The walls were exposed to the standard 834-1 temperature curve for two hours followed by a 24-hour cooling phase. For each stone, one wall was tested unloaded (in practice with a very low mechanical loading in order to ensure a good fit of the wall in the concrete frame) and one with mechanical loading. The applied mechanical vertical loads during the fire test correspond to 50% of the bearing capacity at ambient temperature calculated according to Eurocode 6. In the table and the rest of the paper, the stones from Saint Leu, Tervoux and Massangis are referred to as LEU, TER and MAS respectively. The unloaded and loaded tests are denoted by NL and L.
The recordings were made during the heating and cooling phase. At the end of the cooling phase, the walls were loaded again until failure in order to determine their residual bearing capacity. The walls were stored for at least 2 weeks for further observations.

3. TEST PROCEDURE

The walls were erected by Rocamat company within a reinforced concrete frame. The blocks sizes were: 72 cm x 36 cm x 20 cm (length x height x thickness). The mortar layer thickness was: 10 mm. A layer of mortar was applied between the wall and the top and bottom beams. Their thickness was respectively of 55 mm and 20 mm. A 60 mm-wide rock wool strip was positioned between each lateral side of the wall and the RC frame in order to ensure thermal insulation and prevent any mechanical action on the lateral sides of the walls (free edges).
To accurately characterize the behavior of masonry walls in fire situations, we employed a comprehensive instrumentation and measurement protocol that enabled us to monitor the temperatures, displacements and visual changes: thermocouples, displacement sensors, digital image correlation (DIC), thermal camera and endoscopes (Figure 1).
The structure was placed in front of a furnace and exposed to a conventional ISO 834-1 fire (EN 1991-1-2) on one side for 120 minutes according to NF EN 1365-1. The temperature was uniformly increased on the surface of the wall until it reached 1050°C after 120 minutes (Figure 2). The wall was held against the furnace during the cooling phase. During this phase, the exhaust fans were kept running at high speed and openings were made in the sealing of the furnace to accelerate the cooling rate. During both phases, the temperatures in the furnace were measured using 9 plate thermometers positioned 10 cm from the walls. An example of the results is given in Figure 2.

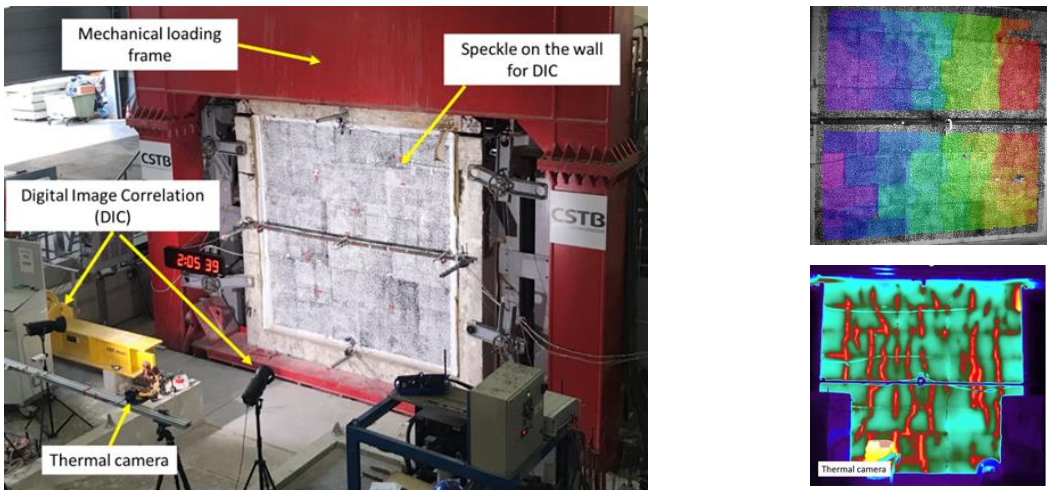

Figure 1: Fire resistance test on the Massangis stone block wall with the cameras of the digital image correlation, the thermal camera, the speckles applied on the wall, the mechanical loading frame (left). Example of contours of horizontal displacement in the non-exposed side after 120 minutes of heating (right top). Example of image captured with the thermal camera. The higher temperature at the cracks are visible (rigth bottom).

Vertical compressive load was applied through hydraulic jacks placed under a reinforced concrete frame. A mechanical loading test was carried out the next day to determine the residual capacity of the wall.
In each wall, 3 stones were instrumented with 6 thermocouples positioned at different depths from the face exposed to the fire: 1, 2, 5, 8, 12 and 17 cm. The evolution of temperature fields of the unexposed side was recorded by using 5 thermocouples and a thermal camera.

Three different techniques were employed to accurately measure the masonry wall displacement during the test. Seven Linear Variable Differential Transformers (LVDTs) were placed at different heights and locations on the non-exposed side of the wall to measure the out-of-plane displacement. Additionally, the vertical displacement of the wall at the top of both the right and left sides were recorded using two sensors. Furthermore, the Digital Image Correlation (DIC) technique was used to obtain displacement fields in three directions of the wall using two cameras, without any contact. To achieve this, a painted speckle pattern was applied to the unexposed surface of the wall, which enabled the system to determine the displacement of a set of points by comparing pictures taken at two different times. The position of the two cameras was calibrated before the test to calculate the displacements in the three directions by triangulation. The measurements obtained using these techniques facilitated the wall determination of the deflection, displacement, cracks and other relevant data.
In addition to all these measurements, the endoscopic cameras were placed inside the furnace to film the changes that occurred to the exposed surface during the heating.

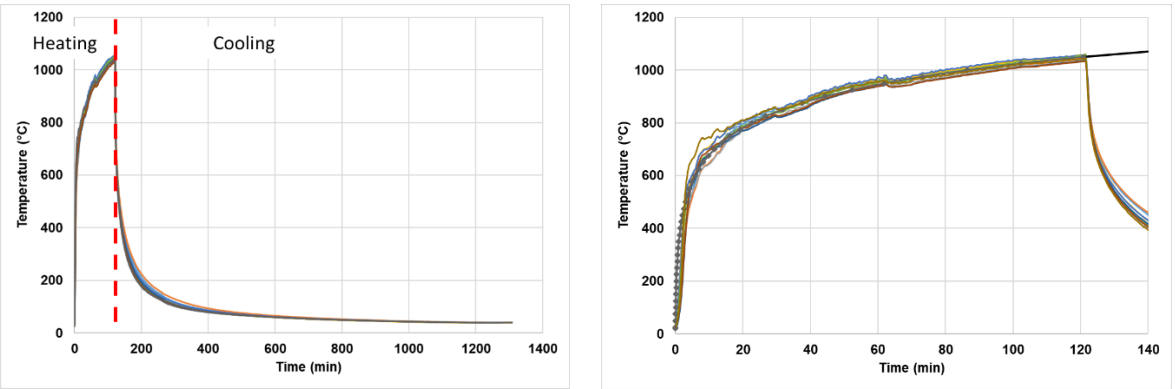

Figure 2: The measured temperature in the furnace during the heating and cooling phase in comparison to the ISO 843-1 curve for the test 3, Unloaded Tervoux

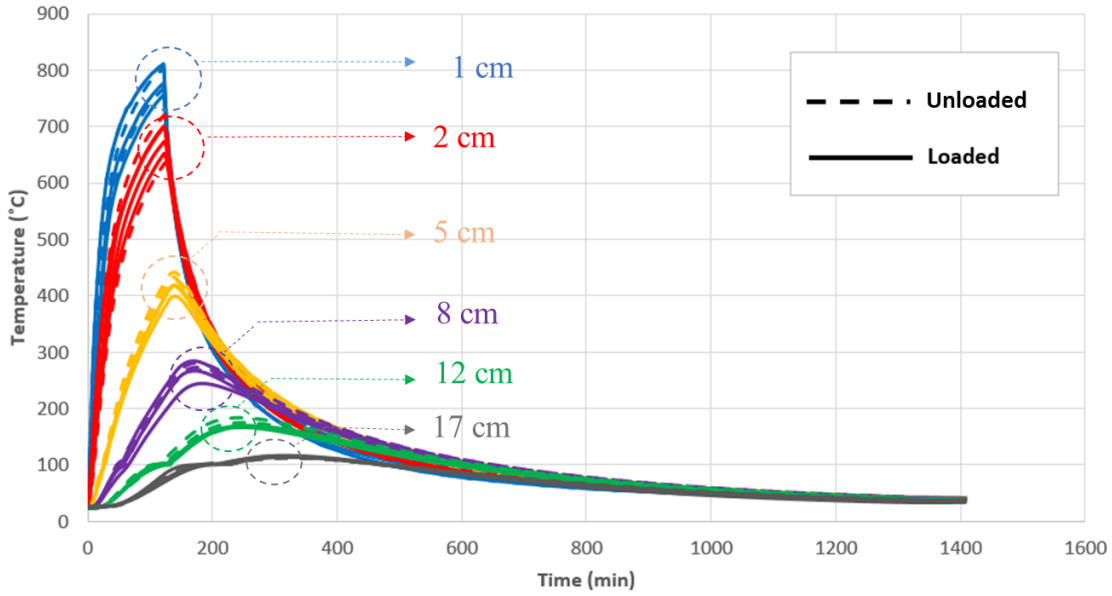

Figure 3: Measured temperature in the wall versus the time and the distance to the exposed side (example of the 2 Tervoux walls)

4. TEST RESULTS AND DISCUSSION

4.1 Temperature distribution

The measured temperature in the wall versus the time and the distance to the exposed side are illustrated in Figure 3. This graph shows the temperatures in both unloaded and loaded Tervoux limestone walls. This graph is representative of the results obtained on the other two walls.

For depths greater than or equal to 8 cm, we can observe the appearance of a vaporization plateau. This type of plateau is frequently observed during fire tests on concrete specimens. The length of the plateaus is less than that observed during tests on Saint-Vaast walls [14]. This can be explained by the longer drying time and the lower water content in the stone in the walls tested in this project. These plateaus result from the energy consumed by the water from the exposed surface to the depth of the measurement. Therefore, the presence of the plateaus, and their length increases with depth.
We can observe that the curves show a greater dispersion of results at shallower depths. This is due to the positioning errors of the thermocouples. Indeed, near the surface, the temperature measurements are more sensitive to positional deviations.

The Figure 4 represents the profiles of temperatures versus the distance to the exposed side determined on the 6 walls at 2 different times: 15 min et 120 min. The actual depths (not the theoretical depths) are plotted on the x-axis. This representation allows the effect of the thermocouple position error to be eliminated and the profiles obtained for the three stones under the 2 mechanical loadings to be compared.
The analysis shows that, for each of the 3 stones, and as expected, mechanical loading has no influence on the temperature profiles.
Although in this representation, the temperatures of the 3 stones are very close at both test times we can observe a trend. The measured temperatures are generally ordered as follows: Saint-Leu, Tervoux and Massangis from the lowest to the highest temperatures.
This agrees with the thermal conductivity measurements determined on the 3 stones [16]. This is also consistent with the compactness and compressive strengths of the limestones (Table 1).

4.2 Out-of-plane displacement distribution

Masonry walls out-of-plane displacement and deflection can fluctuate significantly in response to high temperatures. In the situation of high temperatures, the limestones experience thermal expansion. Because of the temperature gradient, this thermal expansion varies through the thickness of the wall, which leads to an increase in their overall deflection. Such a deflection, also known as thermal bowing, tends to add additional bending moments to the initial compressive stresses borne by the wall, which might trigger its collapse.

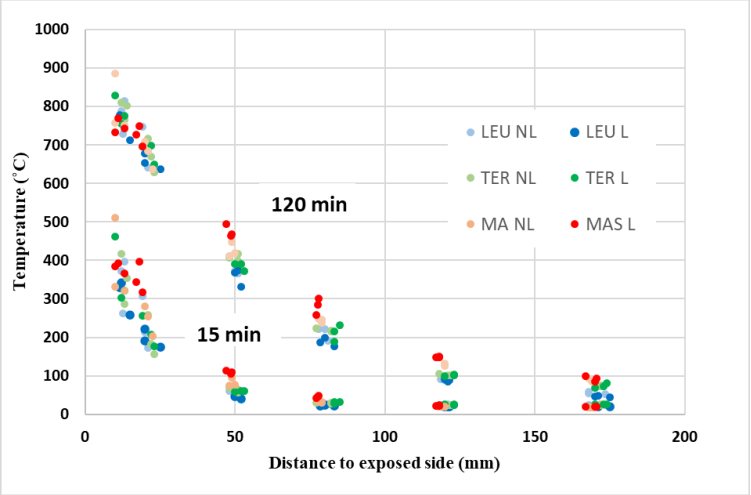

Figure 4: Profile of temperatures versus de depths determined on the 6 walls after 15 and 120 minutes.

The deflection values of the walls during heating and cooling were determined by using five LVDTs and DIC techniques. Positions of the LVDTs are shown in Figure 5-left. Out-of-plane displacement in the middle of the wall versus the time during the heating phase and the beginning of the cooling phase are displayed in the Figure 5-right. Among all the LVDTs, the ones placed in the middle of the wall recorded the maximum out-of-plane displacement in all cases.

Moreover, the results indicated that the unloaded walls had higher out-of-plane displacement compared to the loaded walls, except for the Saint-Leu limestone walls. Thus, the maximum value of out-of-plane displacement was observed for the unloaded Tervoux wall (39 mm). The deflections of the unloaded walls from largest to smallest are as follows: Tervoux (39 mm), Massangis (33 mm) and Saint-Leu (24 mm). The ones of the loaded walls are: Saint-Leu (27 mm), Tervoux (22 mm) and Massangis (6 mm). The 2 Saint-Leu walls out-of-plane displacement values were very close. This small variation can be attributed to the low difference in load between the “unloaded” and the loaded tests (Table 1). On the contrary, the loaded Massangis wall shows a very low deflection compared to the unloaded wall. This is consistent with the very high load applied to the loaded wall (375 tonnes). The rate of increase of out-of-plane displacement was highest during the first 30 minutes and gradually decreased thereafter (Figure 5).

The DIC method is a versatile tool that can offer important information regarding the out-of-plane displacement of the walls. The contours of out-of-plane displacements in the non-exposed side after 120 minutes of heating in 5 of the walls are displayed in Figure 6. Values from the unloaded Saint wall test are not available due a technical problem. From these figures, it can be observed that the maximal deflection occurs very generally near mid-height or a bit above for all walls. For both Tervoux walls, the maximal deflection did not occur at mid-width but was a bit off-center. This is attributed to the asymmetric development of the major vertical cracks (see below).

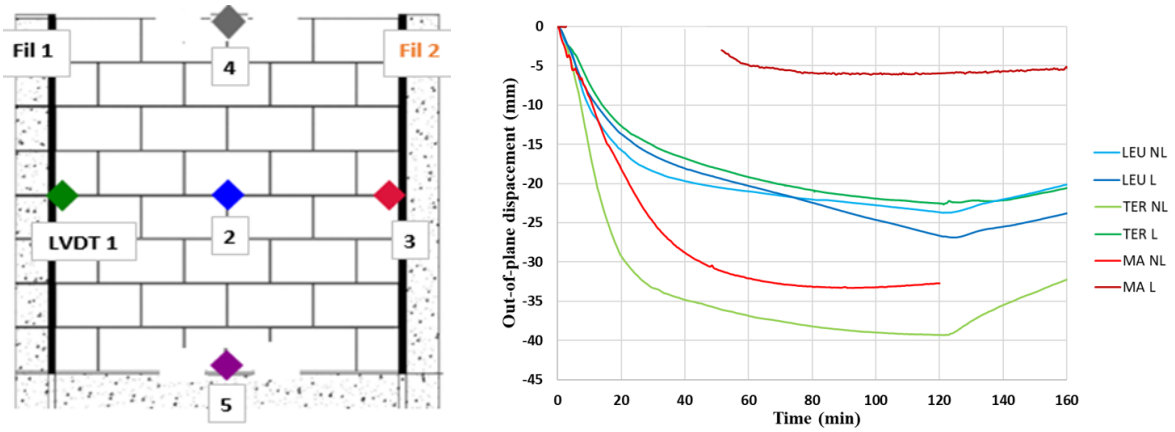

Figure 5: Positions of the LVDTs on the non-exposed side (left); Out-of-plane displacement in the middle of the wall versus the time during the heating phase and the beginning of the cooling phase (right).

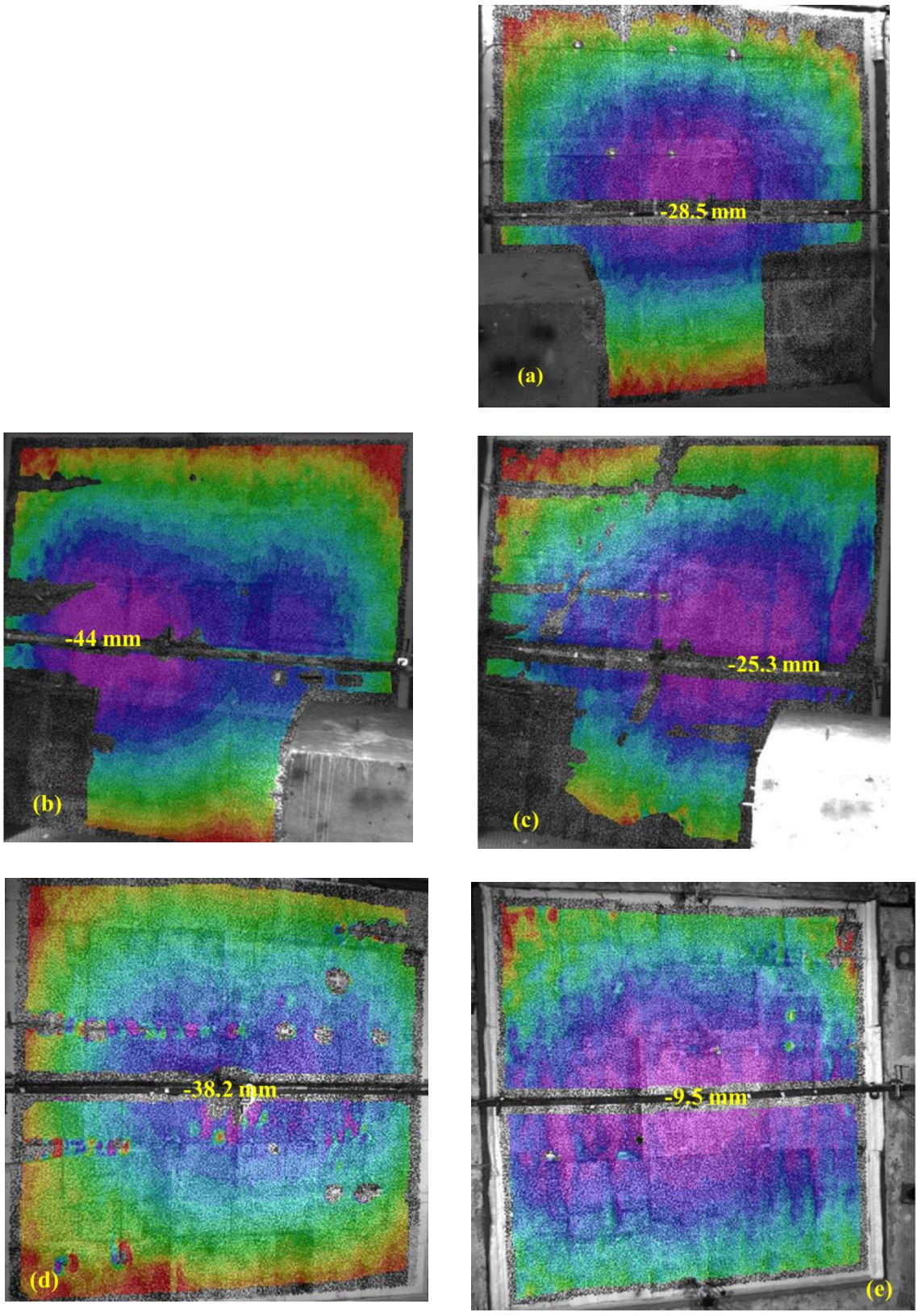

Figure 6: Contours of out-of-plane displacements in the non-exposed side after 120 minutes of heating in Loaded Saint Leu (a); Unloaded Tervoux (b); Loaded Tervoux (c); Unloaded Massangis; Loaded Massangis (e)

In Figure 7, as an illustration, deflection profiles determined from the DIC recorded data on the unloaded Tervoux wall at different times during the heating phase are displayed. Profiles are given along the width at the mid-height (top) and along the height at mid-width (bottom). Curves are compared with the values determined by the 5 LVDTs and represented by colored dots. The results show a relatively good correlation between these two measurement methods. These 2 figures picture well the increase in deflection on both sides during the heating phase. These curves can be usefully compared with those obtained on the Saint-Vaast walls studied by Pham et al [14]. The maximum deflection thus determined after 120 minutes on the unloaded wall was 39 mm.

Figure 8 shows the deflection of the central vertical and horizontal lines of all the walls at the end of the heating phase (120 minutes). These figures also illustrate well the creation of a circular bulge toward the fire.

At the beginning of the cooling phase, the value of out-of-plane displacement started to decrease for all walls. Figure 9 shows a comparison between the values at the end of the heating phase (120 minutes) and the end of the cooling phase (1 day). The ratios between the 2 values are given above in % in the figure. The values are between 6 and 54 %. We can then observe that the deflection is partially reversible. It is almost completely reversible in the case of the unloaded Massangis wall.

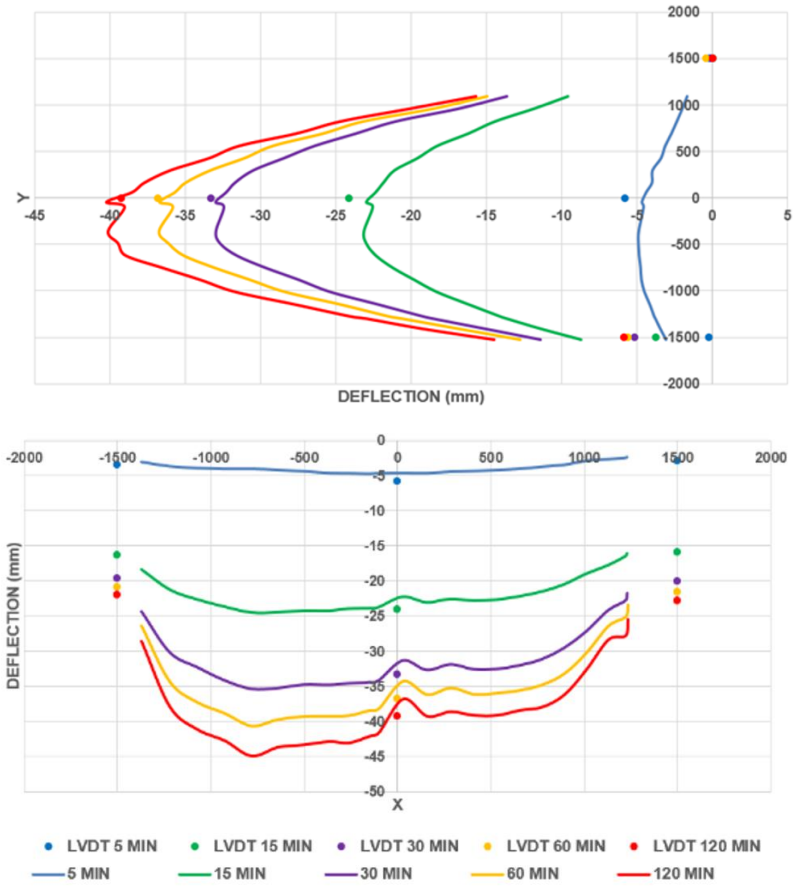

Figure 7: Deflection profiles determined on the unloaded Tervoux wall at different times during the heating phase. Profiles are given along the width at the mid-height (top) and along the height at mid-width (bottom).

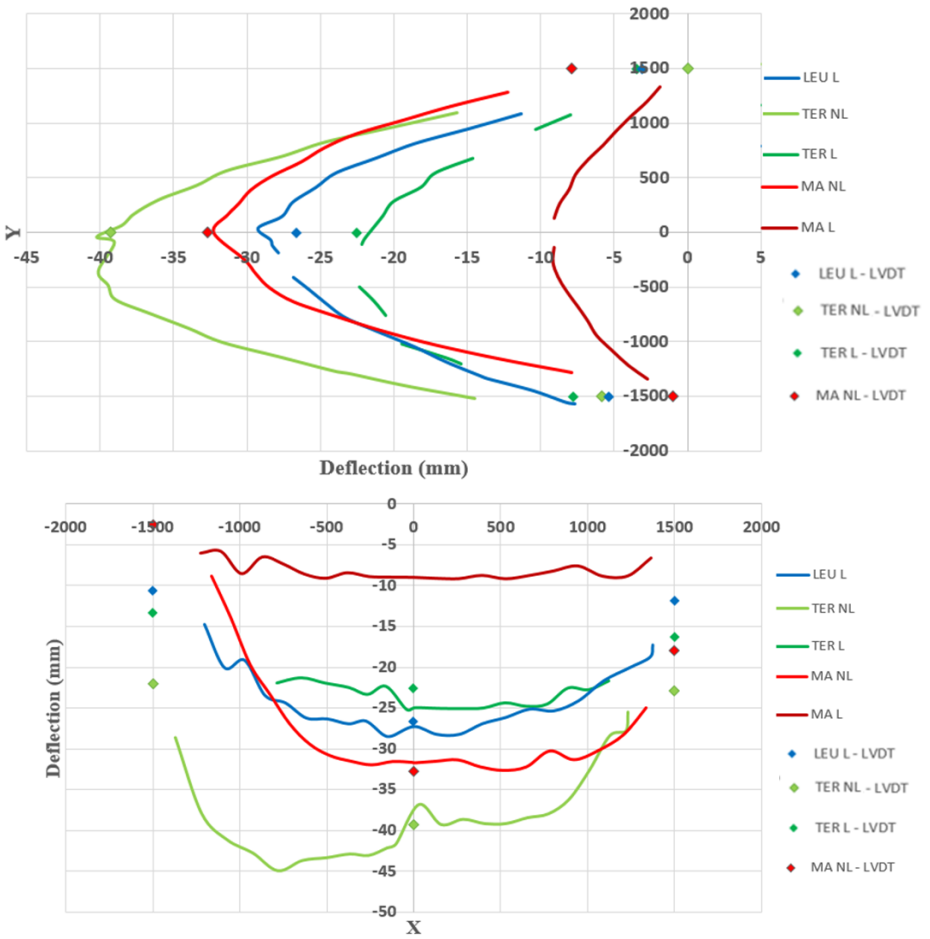

Figure 8: Comparative deflection profiles determined on the walls at the end of the heating phase (120 minutes). Profiles are given along the width at the mid-height (top) and along the height at mid-width (bottom).

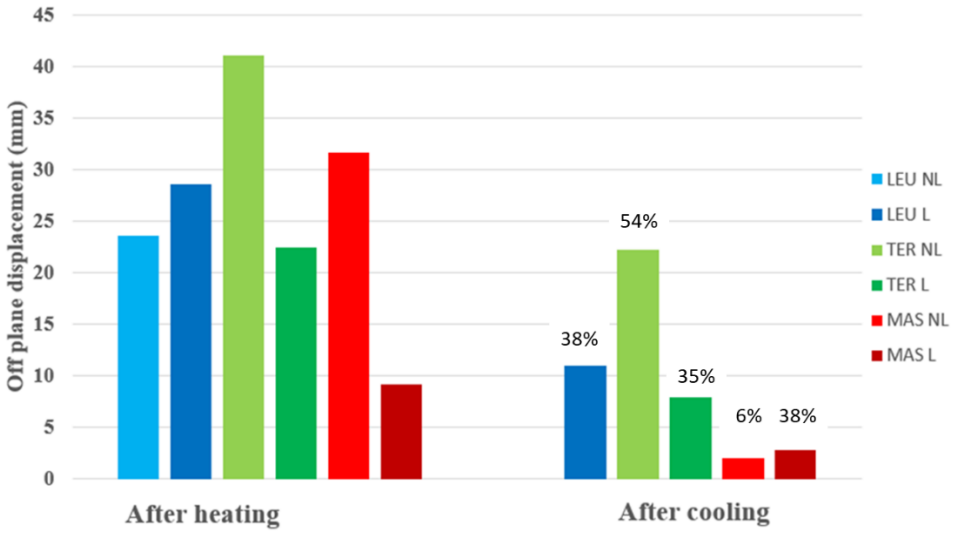

Figure 9: Out-of-plane displacements at the end of the heating phase and at the end of the cooling in all six walls. The ratios between the 2 values are given above in %. All the values have been determined from the DIC measurements except the one determined on the unloaded Saint-Leu wall. This value was determined by LVDT

4.3 Residual load capacity

All six walls, after being subjected to 120 minutes of fire in both unloaded and loaded tests, remained intact and did not fail. To assess their residual mechanical behavior, the day after the heating test, when the temperature in all thicknesses of the walls had stabilized, the walls were loaded again until failure to determine their residual bearing capacity. The compressive vertical load was applied at a gentle speed over ten minutes and increased the load until the walls failed. Values of the calculated load capacity according to Eurocode 6, the applied load during the fire tests and the determined residual capacity are given in the Figure 10. The upward pointing arrows indicate that the applied loads allowed by the equipment used for each test were not high enough to break the walls. Both Saint-Leu walls failed at a load of 100 tonnes. For the Tervoux walls, the wall which was loaded during the fire test wall failed at 200 tones. The unloaded wall was able to withstand a load greater than 200 tonnes. The Massangis walls (unloaded and loaded walls), with the highest compressive strength among the three types of limestone, had a residual capacity exceeding 375 tonnes and did not fail (Figure 10).
These results are among the most important findings of this work. They show that even after fire exposure, the limestones masonry walls can retained a significant amount of their load-carrying capacity.

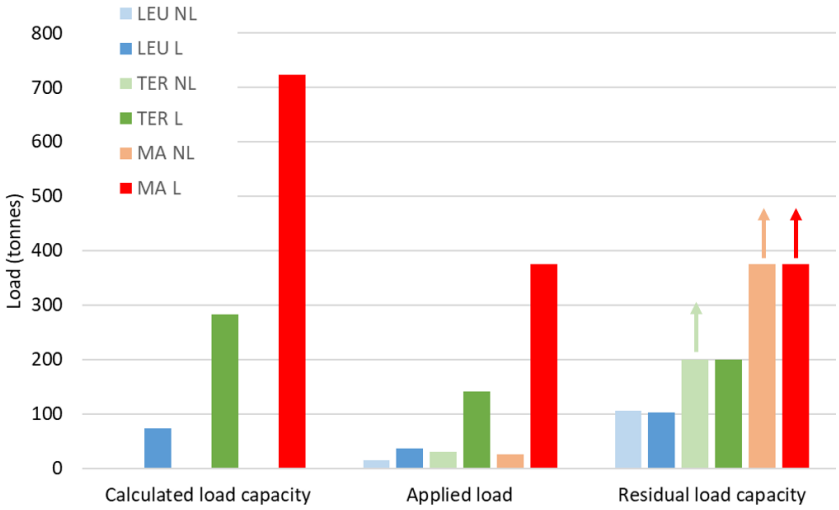

Figure 10: Calculated theoretical load capacity, applied load during heating and residual load capacity after cooling. Arrows are displayed when failure have not been reached when the load was applied after cooling

4.4 Visual changes and cracks during the heating and cooling phases

The evolution of the face exposed to fire was observed and recorded by means of endoscopes. Few changes were observed. In some tests we observed small delamination. None of the three stones exhibited any spalling phenomena.

Cracks development on the unexposed side
The observed cracking patterns on the non-exposed side of the masonry walls after 120 minutes of heating are displayed in Figure 11. It is noteworthy that vertical cracks were prevalent in comparison to horizontal cracks and indeed, in all cases, the cracks emerged from the vertical joints and propagated vertically through the stones, originating from the center of the wall. The first cracks appeared within the first ten minutes of heating in all six tests. The depth of the cracks varied from 5 mm to 17 mm across the length of the wall, and transverse cracks were present in all walls. In loaded walls, the presence of cracks in the top angles and lateral sides was more pronounced compared to not-loaded walls. In some cases, a large horizontal crack was observed at the bottom of the wall, between the blocks and the mortar bed (Figure 11).
The number of vertical cracks was similar in all cases. In most of the cases the number was between 7 and 9. However, we can note that the number of cracks in the case of the Massangis walls was lower (about 6 for the unloaded case) and higher (about 14 for the loaded wall case). Interestingly, these observations can be compared with the horizontal displacement measurements determined by means of the DIC. An example of contours of

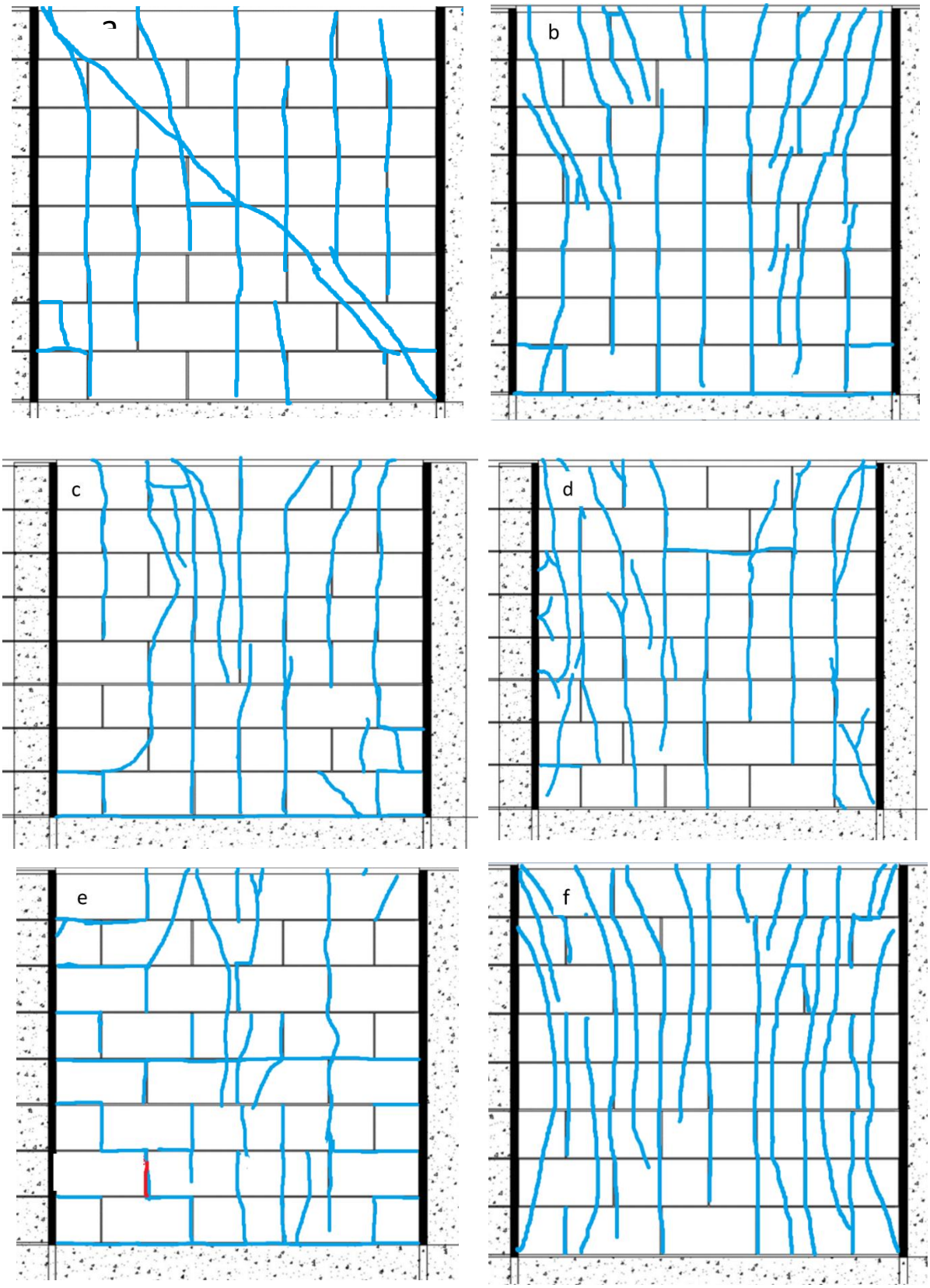

Figure 11: crack patterns on the exposed side of wall after 14 days in Not-loaded Saint-Leu (a); Loaded Saint-Leu (b); Not-Loaded Tervoux (c); Loaded Tervoux (d); Not-Loaded Massangis (e); Loaded Massangis (f)

Figure 12: Pictures of the exposed sides of the walls after 14 days in unloaded Saint-Leu (a); Loaded Saint-Leu (b); Unloaded Tervoux (c); Loaded Tervoux (d); Unloaded Massangis (e); Loaded Massangis (f)

horizontal displacement is given in Figure 1. The measurements showed that the total horizontal elongations for all the walls after 120 minutes of heating were all between 20 and 24 mm. Therefore, the width of the cracks was in the majority of cases of the order of 2.5 mm. In the case of the two unloaded and loaded Massangis walls, they were respectively of the order of 3.5 and 1.7 mm. The images recorded with the thermal camera also allow the visualization of cracks. The cracks show locally higher temperatures during the heating phase (Figure 1). The detailed analyze of the data from the DIC system and the thermal camera which have not been presented in this paper will be presented in a future article.

4.5 Observations after the tests

After one day of cooling and mechanical load assessment, the reinforced concrete frame containing the wall was removed from the furnace to inspect the exposed side of the wall. Figure 12 illustrates the condition of the exposed side of all six walls after 14 days. Notably, the walls that failed due to the applied mechanical load exhibited a more severe cracking pattern. The observations also showed that some stones showed cracking parallel to the plane of the wall. This was particularly noticeable in the Saint-Leu stones. It was relatively easy to detach large blocks of about 3 cm thickness by tapping the surface with a hammer. In addition to the cracks, a visible change in the color of the limestone blocks was observed. Indeed, limestones exposed to high temperatures experienced a color change at different temperatures [7]. For temperatures greater than 730 degrees of Celsius, decarbonization of the calcite in these stones occurs, and upon exposure to the humidity in the air, it transforms into lime and eventually falls apart. Based on the evaluation of temperature distribution across the wall, it is estimated that approximately 1 cm of the thickness of the wall failed during this time.

CONCLUSIONS

In conclusion, this study investigated the behavior of masonry walls made of three different types of limestone with different compressive strengths subjected to fire exposure for 120 minutes, followed by the assessment of their residual capacity. In this paper, we mostly present the study of the out-of-plane displacements, residual mechanical behavior, and cracking patterns of the walls.

The results indicate that the unloaded walls experienced more significant out-of-plane displacement toward the fire – in comparison to the loaded ones - during heating, with the highest displacement occurring in the center of the walls and decreasing along the boundaries. The DIC analyses showed that the out-of-plane displacements for the majority of the tests had relatively high symmetry. However, we have noted that for both Tervoux walls, the maximal deflection did not occur at mid-width but was a bit off-center.

After heating, all six walls remained intact and did not fail. The walls with the higher value of compressive strength, retained a significant amount of their load-carrying capacity, as demonstrated by the residual mechanical behavior tests. The compressive strength of the limestone and the amount of load during heating differed, resulting in varying residual loads for each case. The Massangis walls demonstrating the highest residual capacity exceeding 375 tonnes.

Cracking patterns on the non-exposed side of the masonry walls after 120 minutes of heating showed that vertical cracks were prevalent, originating from the vertical joints and propagating vertically through the stones, more specifically in the center of the walls. Transverse cracks were present in all walls, and in loaded walls, the presence of cracks in the top angles and lateral sides was more pronounced compared to unloaded walls.

In addition, the study found that the exposed side of the walls shows a visible color change of the limestone blocks after exposure to high temperatures. The study estimated that approximately 1 cm of the thickness of the wall failed during heating due to the decarbonization of the calcite in the limestone blocks.

This work highlights the importance of considering the behavior of masonry walls under fire exposure and the potential impact on their load-carrying capacity and structural integrity. Results show that, even after fire exposure, the limestones masonry walls can retain a significant amount of their load-carrying capacity. which can inform the development of more resilient and fire-safe building designs.

Supplementary analysis of the experimental data (DIC system, thermal camera …) which have not been presented in this paper and numerical simulations of the effect of high temperature on the behavior of limestone masonry walls are under way and will be presented in future articles.

Acknowledgement

The authors want to acknowledge the contribution of all the partners of the French POSTFIRE project for the fruitful technical discussions. We want to particularly acknowledge the company Rocamat to provide the limestone blocks and erect the walls and the CSTB team involved in carrying out the tests. Special acknowledge is addressed to M S. Charuel, M. Cruz and L. Gontier.
Finally, the authors acknowledge the French National Research Agency (ANR) for their financial support.

REFERENCES

[1] Gomez-Heras M, Mc Cabe, S. et al. (2009). Impacts of fire on stone-built heritage – An overview. Journal of Architectural Conservation 15(2):47-58
[2] Mertz, J. D., Colas, E., Ben Yahmed, A., Lenormand R (2016). Assessment of a non-destructive and portable mini permeameter based on a pulse decay flow applied to historic surfaces of porous materials. In: Proc. of the 13th International Congress on the deterioration and conservation of stone, 6-10th September 2016, Paisley, Scotland.
[3] Comité Européen de Normalisation (2007). EN 1996-1-2: 2007 – Design of masonry structures – Part 1-2: General rules – Structural fire design.
[4] National fire Protection Association (2019). NFPA® 914 Code for the Protection of Historic Structures, 2019 Edition. Available at https://www.nfpa.org/codes-and-standards
[5] Ingham, J. P. (2009). Application of petrographic examination techniques to the assessment of fire-damaged concrete and masonry structures. Materials Characterization 60:700-709.
[6] Sippel, J., Siegesmund. S., Weiss, T., Nitsch, K. H., Korzen, M. (2007). Decay of natural stones caused by fire damage. In: Přikryl R and Smith BJ (eds.), Building stone decay: from diagnosis to conservation. Geological society of London, Special Publications, 271:139-151
[7] Vigroux, M. (2020) Influence de la microstructure et de la minéralogie sur l'endommagement mécanique des pierres de construction utilisées dans le patrimoine bâti sous l'effet de conditions environnementales sévères, PhD Thesis, Université de Cergy Pontoise, 399 p.
[8] Koca, MY, Ozden, G, Yavuz, A. B. et al. (2006). Changes in the engineering properties of marble in fire-exposed columns. International Journal of Rock Mechanics & Mining Sciences, 43:520-530
[9] McCabe, S, Smith, B. J., Warke, P. A. (2010). Exploitation of inherited weakness in fire-damaged building sandstone: the 'fatiguing' of 'shocked' stone. Engineering Geology, 115:217–225
[10] Russo, S, Sciarretta F (2012). Experimental and theoretical investigation on masonry after high temperature exposure. Experimental Mechanics, 52:341-359
[11] Russo, S, Sciarretta F (2013). Masonry exposed to high temperatures: Mechanical behaviour and properties – An overview. Fire Safety Journal, 55:69-86
[12] Wu, Q., Weng L et al. (2019). On the tensile mechanical characteristics of fine-grained granite after heating/cooling treatments with different cooling rates. Engineering Geology 253:94-110
[13] Ghobadi, M. H., Babazadeh, R. (2015). Experimental studies on the effects of cyclic freezing–thawing, salt crystallization, and thermal shock on the physical and mechanical characteristics of selected sandstones. Rock Mechanics and Rock Engineering, 48:1001-1016
[14] Pham, D. T., Donval, E., Pinoteau, N., Pimienta, P., Pallix, D. (2022). Test of loaded and unloaded natural stone masonry walls exposed to fire, Materials and Structures/Materiaux et Constructions, 55/9, November 2022, art. 229
[15] Donval, E., Pham, D.T., Hassen, G., de Buhan, P., Pallix, D. (2022) Essai de résistance au feu d'un mur en maçonnerie en pierre naturelle. Academic Journal of Civil Engineering : Proceedings of the 40th meeting of universities in civil engineering (RUGC) - Lille.10.26168/AJCE.40.1.50
[16] Daoudi, A., Sciarretta, F., Eslami, J., Beaucour, A. L., Noumowé, A., Experimental characterization of physical, thermal, transport and mechanical properties of 13 french limestones, Construction and Building Materials (under review).